Spatial coherence analysis of intense ultra-flat white laser*

YANG Lan[1,2], LIU Junming[3,2], HONG Lihong[1,2], LIU Liqiang[1,2], LI Zhiyuan[1]

1.School of Physics and Optoelectronics, South China University of Technology, Guangzhou 510640, China

2.Jingqi Laser Technology Corporation Limited, Dongguan 523808, China

3.School of Integrated Circuit, South China University of Technology, Guangzhou 510640, China

Abstract

White light is typically considered incoherent; however, the recently popular supercontinuum laser, also known as white laser, spans the visible spectrum and features high laser intensity and good coherence, challenging this traditional limitation. The white laser has a wide range of applications, including multi-channel confocal microscopy, color holography, and white light interferometric surface topography. Although white lasers have been proposed and developed extensively in terms of technology, specific analyses of their optical wave properties—especially spatial coherence—are still lacking. Since many applications impose certain requirements on the spatial coherence of white light, the lack of research into the spatial coherence of white lasers has, to some extent, limited their practical use. This paper presents a detailed experimental study and analysis of the wavefront intensity, polarization characteristics, and spatial coherence of the high-intensity ultra-flat spectrum white laser that was independently developed by our research group in 2023. The laser is generated by broadening the spectrum of a high-intensity Ti: sapphire femtosecond laser through second- and third-order nonlinear effects. A bandpass filter is used to extract eight components from the white laser, with a central wavelength range from 405 nm to 700 nm and a bandwidth of 10 nm for each component. By measuring the performance of these eight quasi-monochromatic lasers, the characteristics of the white laser of the entire visible spectrum can be evaluated. The CCD imaging of the collimated quasi-monochromatic laser spots reveals that their wavefront intensities exhibit a quasi-Gaussian distribution with uniform beam profiles. Polarization measurements by using polarizers at various angles show that the white laser is linearly polarized. A Young's double-slit interferometer is used to

---

* The paper is an English translated version of the original Chinese paper published in Acta Physica Sinica. Please cite the paper as: **YANG Lan, LIU Junming, HONG Lihong, LIU Liqiang, LI Zhiyuan, Spatial coherence analysis of intense ultra-flat white laser.** Acta Phys. Sin., 2025, 74(12): 124201. doi: 10.7498/aps.74.20250373

measure the interference fringe contrast of the eight quasi-monochromatic beams to assess their spatial coherence. The experimental results show that the average interference fringe contrast of the entire visible spectrum is 0.77, and the difference between different wavelengths is very small. This indicates that the white laser has excellent spatial coherence in the visible range. The eight quasi-monochromatic lasers in the visible spectrum all exhibit quasi-Gaussian wavefront intensity distributions, linear polarization, and high spatial coherence. This indicates that the white laser inherits the excellent properties of the Ti: sapphire laser. All of these data provide valuable guidance for the application of white lasers in color holography, white light interferometric surface tomography, microscopic imaging, and other fields that require white light with a certain degree of coherence.

Keywords: white laser, spatial coherence, interference fringe visibility

PACS：42.25.Kb,42.25.Hz,42.65.–k,42.55.–f

doi: 10.7498/aps.74.20250373

cstr: 32037.14.aps.74. 20250373

1. Introduction

White laser is a kind of supercontinuum laser. Supercontinuum laser refers to a laser with an ultra-wide spectral band of hundreds to thousands of nanometers[1–3]. White laser refers to a supercontinuum laser whose spectral band covers the visible band. Supercontinuous laser is usually generated by focusing a narrow incident pulse into a medium so that the local intensity is high enough to excite a variety of nonlinear effects in the medium[4]. Common nonlinear mechanisms include optical soliton effect,[5,6], four-wave mixing,[7], Kerr effect,[8,9], and self-phase modulation (SPM)[10–13]. In the past 10 years, our group has systematically developed white laser technology based on Ti: sapphire femtosecond laser[14–20]. In these schemes, the white laser is generated by a Ti: sapphire femtosecond laser through a variety of nonlinear effects, which can obtain an ultra-wide spectral band while retaining the characteristics of the laser, such as high intensity and coherence. Such light sources have broad application prospects in many fields. Among them, multi-channel confocal microscopy, white light interferometry and color holographic three-dimensional display are three key potential applications, which are worth further exploration. Multi-channel confocal microscopy is a high-precision color microscopic imaging technique, which usually requires high-intensity laser and can quickly switch the wavelength[21]. White lasers can switch wavelengths more easily and provide more colors than traditional multi-color laser integration schemes. White-light interferometry is a technique for high-precision three-dimensional surface topography measurement by interference using a broad-spectrum light source[22]. Compared with traditional white light with poor coherence, such as LEDs or halogen lamps, white laser can significantly improve the resolution and enhance the noise immunity in this

application. In addition, color holographic[23] is considered to be the "holy grail" of three dimensional (3D) display technology, and its principle is to record and reconstruct the 3D wavefront of light using interference fringes. Compared with the traditional monochromatic laser (whose holograms can only appear monochromatic), the white laser covers the entire visible spectrum, making color holography possible, which can not only expand the color range, but also improve the color accuracy of holograms.

In these applications, white light interferometry and color holography require white light to have interference ability. Good spatial coherence is the necessary prerequisite for the realization of interference imaging, and is the key factor to determine the performance and feasibility of white laser. Therefore, researchers must consider the spatial coherence of white laser when choosing it as a light source. However, although many supercontinuum lasers have been proposed, there is almost no research on the measurement and analysis of the spatial coherence of these supercontinuum lasers. Among the few previous studies, only the wavefront of supercontinuous laser was analyzed. In 2018, Kueny et al.[24] analyzed the wavefront of a white supercontinuum laser. The experimental results show that the wavefront deformation of the laser is serious, the spot is non-circular and the spot intensity distribution is uneven. There are also a few studies that only simulate and analyze the coherence, but do not carry out actual measurements and provide specific measurement data. For example, Genty et al. Proposed a theoretical model to analyze the spatial coherence of white laser[25]. The coherence properties of supercontinuum laser pulses are studied by using the second-order coherence theory of nonstationary light. It is shown how to construct the second-order correlation function in the time domain and frequency domain by numerical simulation of a collection of single pulses, and two convenient mode representations are proposed. This study only stays in the theoretical simulation analysis, and still does not carry out the actual measurement. Melnik et al. Established a mathematical model[26] to analyze the temporal coherence of supercontinuum laser. Through theoretical analysis and numerical simulation, it is revealed that the coherence time of the continuum depends on the different parameters of the input pulse, which can be attributed to the relationship between the coherence time and the phase modulation coefficient. But this is still a study that stays at the stage of simulation analysis. The only study involving actual measurement is a study on the measurement of the coherence length of a supercontinuous laser. The coherence length of a supercontinuous laser at 550 nm center wavelength was measured to be 1.6 μm by Zeylikovich and Alfano[27]. However, this study only analyzed the temporal coherence of a single supercontinuum wavelength, and did not measure the spatial coherence of the whole supercontinuum spectrum.

To sum up, although many white lasers (supercontinuum lasers) have been proposed in recent years, their wide spectral band characteristics have also been mentioned and verified in many

studies[28–32]. However, there is a lack of research on the measurement and analysis of their beam properties as lasers, such as wavefront, polarization, and coherence. In particular, the coherence of white laser has not been verified. This will limit the practical application of white laser. In order to solve this important problem in basic optics and applied physics, the spatial coherence properties of a high intensity ultra-flat band white laser developed by our group in recent years were analyzed[18–20]. As shown in the Fig. 1, the generation principle of the white laser is briefly introduced, and the theoretical support of white laser with white light and laser characteristics is provided. Then experiments are designed to measure the wavefront intensity characteristics, polarization characteristics and spatial coherence of white laser. The measurement results show that the white laser inherits the wavefront intensity characteristics of the Ti: sapphire femtosecond laser, and has a quasi-Gaussian wavefront intensity distribution and a uniform spot distribution. The polarization of white laser is linear polarization, which is the obvious characteristic of laser. Finally, the experimental setup of Young's Young's double interferometer (YDSI) is set up, and the interference fringes are generated by the eight components of white light in the visible band, respectively. The average contrast of these fringes is measured to be 0.77, which indicates that the white laser has good coherence. The three experimental results all prove that the white laser has the characteristics of both white light and laser, which provides a strong reference for the application of white laser in the field requiring the use of white light with high intensity coherence. The results of this experiment will promote the practical application of white laser, an excellent light source, in various fields and promote the development of various industries.

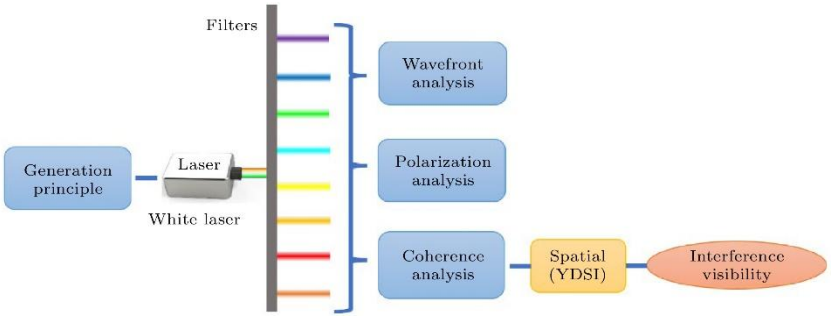

Figure 1. Analysis scheme of laser characteristics such as spatial coherence of white laser.

2. Generation principle and spectral characteristics of white laser

White laser is a kind of supercontinuum laser with ultra-wide spectral band. Supercontinuum laser whose spectrum covers the whole visible band is also called white laser. White laser is mainly produced by nonlinear effect. The most common methods include a variety of third-order nonlinear (3rd-NL) effects, such as self-phase modulation (SPM), four-wave mixing, and stimulated Raman scattering, which are usually realized in microstructure devices such as photonic crystal fiber (PCF)[8]. However, when relying solely on the third-order nonlinear effect for spectral broadening, there are often limitations in spectral flatness and

energy distribution. For example, in the broadened spectrum, the energy near 400 nm is low, while the energy at 800 nm (the center wavelength of the Ti: sapphire femtosecond laser) remains high, resulting in an obvious uneven distribution of the whole spectrum, and the farther the wavelength is from the center wavelength, the lower the energy is. This imbalance limits the simultaneous optimization of spectral bandwidth, flatness, and pulse energy.

In the past decade, our group has proposed and developed a new method to generate femtosecond white laser by combining second-order (2nd-NL) and third-order nonlinear effects[14–20]. By optimizing the individual functions of the 2nd-NL and 3rd-NL effects and their synergistic effects, a high-performance femtosecond white laser is finally realized[20]. The laser has high pulse energy (~ 1.1 mJ), ultra-wide bandwidth and ultra-high spectral flatness (3 dB attenuation spectral bandwidth covering 385 — 1080 nm, spanning the near ultraviolet, visible and near infrared regions).

In order to better understand the performance of the white laser, Fig. 2(a) demonstrates its generation principle and process. In this experimental setup, a Ti: sapphire femtosecond laser is used as the pump source (pulse energy up to 4 mJ, central wavelength of 800 nm, pulse width of about 50 fs, repetition rate of 1 kHz). First, the beam is focused by lens 1 into fused silica, and then focused by lens 2 into a chirped periodically polarized lithium niobate (CPPLN) crystal. The structural parameters of the CPPLN crystal are specially designed according to the output characteristics of fused silica, and the CPPLN crystal and the fused silica complement each other in parameter configuration to achieve optimal synergy and achieve excellent spectral broadening effect[20]. It should be emphasized that the high-performance femtosecond pulse laser used in this experiment is completely developed by our research group.

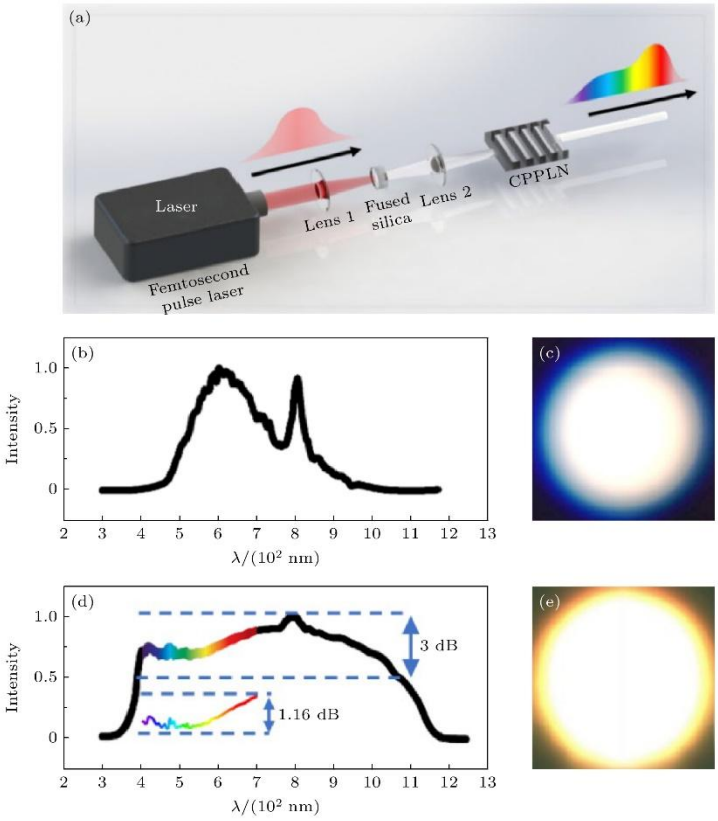

Figure 2. Basic information of the white laser: (a) Schematic diagram of a homemade femtosecond white laser created by sending an intense Ti: sapphire femtosecond pulse laser beam through a fused silica-CPPLN 2nd-NL and 3rd-NL synergistic nonlinear frequency conversion module. (b) The measured spectrum of the light after the fused silica plate. (c) The spot of the laser after the fused silica plate. (d) The measured spectrum of the white laser shows the ultra-flat spectral profile. The color band represents the visible range, whose enlarged view is shown in the inset. (e) The spot of the white laser beam.

In the experiment, an ordinary fused silica plate (thickness 8 mm) is used to achieve the third-order nonlinear broadening. The SPM effect plays the most important role in the broadening process, which broadens the input Ti: sapphire femtosecond laser (3 dB spectral bandwidth of 20 nm) to a supercontinuous white laser with a 3 dB spectral bandwidth of about 300 nm. The spectrum and spot behind the fused silica plate are shown in Fig. 2(b),(c), respectively. The spot has a blue hue due to the depression of the red band. In order to further broaden the spectrum and enhance the energy distribution over the whole bandwidth, a self-developed CPPLN thin plate crystal (length 20 mm, thickness 2 mm, width 6 mm) was used to achieve quasi-phase matching. The crystal uses the second-order nonlinear effect to effectively convert and redistribute high-energy spectral components, so that the energy distribution can be adaptively adjusted, thereby significantly improving the spectral flatness. The spectrum and spot after CPPLN are shown in Fig. 2(d)and(e), respectively. From the Fig.

2(d)and(e), it can be seen that the final output signal laser from the fused silica-CPPLN cascade nonlinear optical module is a broad-band, spectrally flat white femtosecond laser.

The Fig. 2(d)shows the measured spectrum of the white laser developed by our group, and its 3 dB bandwidth covers 385 — 1080 nm, which indicates that the white laser has an ultra-wide 3 dB bandwidth of nearly 700 nm and exhibits ultra-flat spectral characteristics. The Fig. 2(d)illustration further shows that the white laser has better spectral flatness in the visible band (400 — 700 nm), and the spectral fluctuation is only 1.16 dB in the bandwidth of 300 nm, which achieves extremely high flatness. The Fig. 2(e)shows the spot of the white laser as a balanced white light with a yellowish tint. This is mainly due to the increased intensity of red light, which makes it look similar to natural sunlight. In addition, the average spectral energy intensity of the white laser in the visible range is measured to be 1.45 μJ/nm (or about 14.5 μJ in a 10 nm bandwidth), and the spectral power intensity can even reach about 30 MW in a 10 nm bandwidth. This is a fairly high spectral intensity level for white light and even white laser light.

3. Experimental measurement and results of white laser beam characteristics

3.1 Analysis of Wavefront Intensity Characteristics of White Laser

In the experiment, eight filters are used to extract eight quasi-monochromatic waves from a white laser. The specific parameters are shown in Tab. 1. The central wavelengths of the eight filters are 405 nm, 450 nm, 500 nm, 532 nm, 580 nm, 600 nm, 635 nm and 700 nm, respectively, covering the entire visible spectral range, corresponding to colors from purplish blue, blue, cyan, green, yellow, orange to red. Due to the high price of ultra-narrowband filters (such as 1-3 nm band-pass filters), a filter with a bandwidth of 10 nm was used in this study to extract light waves with different wavelengths. In this way, eight quasi-monochromatic laser beams can be obtained in a simple way based on this high-performance, ultrashort pulse, high intensity and extremely flat spectrum white laser. The performance of these quasi-monochromatic lasers will well reflect the overall characteristics of white lasers.

Table 1. Central wavelength and bandwidth of the filter used to extract the light wave from the white laser.

	Wavelength/nm							
	405	450	500	532	580	600	635	700
Bandwidth/nm	10	10	10	10	10	10	10	10

In this study, the wavefront intensity morphology of each selected quasi-monochromatic laser beam was first measured. Images of the collimated beam wavefront intensity are captured by a Canon digital camera and displayed in a Fig. 3(a)—(h). On the right side of each wavefront

image, there are two line plots: the middle plot shows the line intensity distribution of the corresponding spot, and the rightmost plot depicts the spectral distribution. These images show that each beam forms a high-quality quasi-Gaussian wavefront intensity, which is highly similar to the excellent Gaussian wavefront intensity of the femtosecond pumping laser of Ti: sapphire. In addition to the good shape of the circular spot of the beam profile, the color uniformity of each selected light wave over the entire beam cross-section is excellent, showing no significant maldistribution. This excellent wavefront quality indicates that the white laser developed by the macroscopic nonlinear frequency conversion and spectral broadening module exhibits excellent uniformity over the entire frequency range. The Fig. 3 show that the macroscopic nonlinear optical module can not only effectively maintain the wavefront intensity characteristics of the pump light, but also achieve its design goals of frequency conversion and spectral broadening, thus showing excellent overall performance. Therefore, it is reasonable to expect that the white laser also retains the excellent spatial coherence of the pump femtosecond laser.

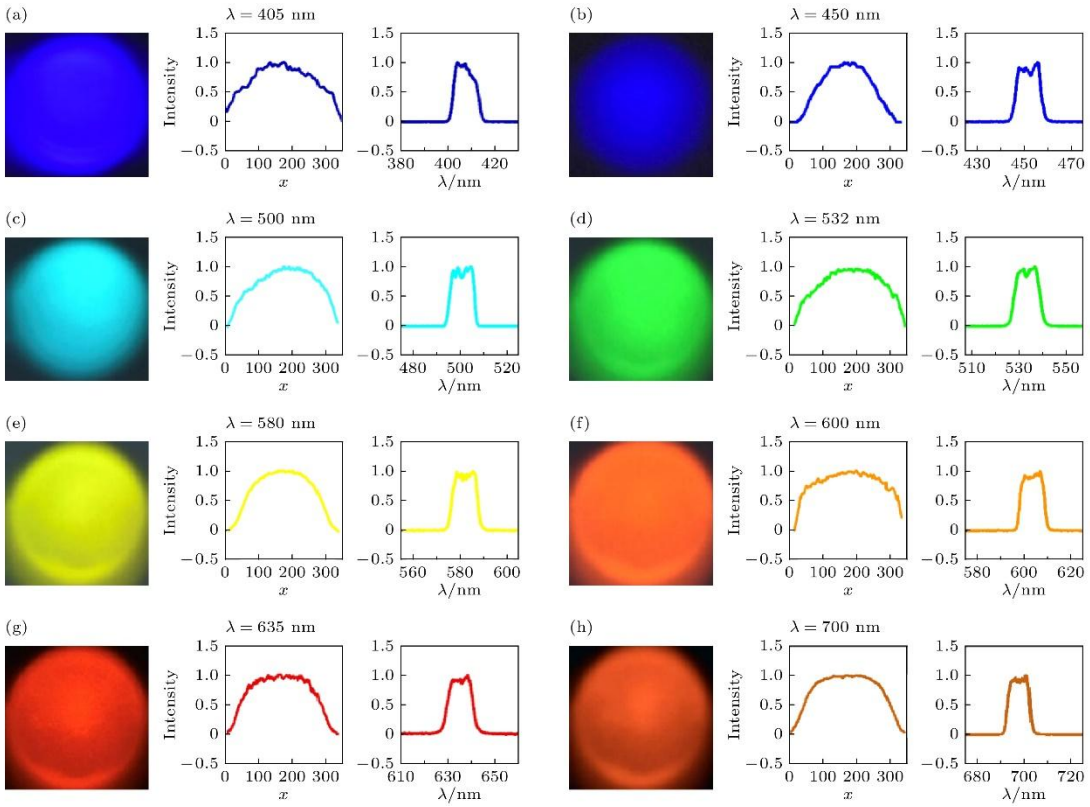

Figure 3. Wavefront analysis. Wavefront (left), line profile (center), and spectral profile (right) of the white laser at different spectral components in the visible band when it passes through 10 nm bandwidth filters centering at the wavelength of (a) 405 nm, (b) 450 nm, (c) 500 nm, (d) 532 nm, (e) 580 nm, (f) 600 nm, (g) 635 nm, and (h) 700 nm

3.2 Analysis of Polarization Characteristics of White Laser

Polarization is also one of the important properties of lasers. A good laser is usually linearly polarized. Therefore, in addition to the coherence analysis, the polarization characteristics of white laser are also analyzed in this study, and the power of eight quasi-monochromatic waves passing through the polarizer is detected by an optical power meter. There is an attenuator behind the polarizer to control the maximum output optical power below the maximum value of the optical power meter. When the polarizer is rotated, the power changes. For each wavelength, record the maximum and minimum powers and their corresponding angles. See.. for specific data Tab. 2. In this study, it was found that the difference between the maximum power and the minimum power was more than 100 times, and all the angles corresponding to the maximum power were mainly concentrated at 0 °, with only a few wavelengths slightly deviated by 1 °. Therefore, according to Malus' law, the white laser can be considered to have good linear polarization properties. This result once again verifies the excellent performance of the white laser in our group.

Table 2. Power variation with polarizer angle for each quasi-monochromatic light after filtering.

	λ/nm							
	405	450	500	532	580	600	635	700
$I_{max}/\mu W$	43.7	42.5	43.5	40.1	45.7	46.8	45.0	46.2
$\theta_{max}/(°)$	0	0	1	0	1	0	0	0
$I_{min}/\mu W$	0.2	0.2	0.1	0.1	0.2	0.2	0.2	0.2
$\theta_{min}/(°)$	90	90	89	90	89	90	90	90

3.3 Analysis of spatial coherence of white laser

The evaluation of the spatial coherence of a white laser requires interference fringes visibility, and the standard experimental setup for this is the famous YDSI. The laser beam passes through the two slits of the YDSI to produce two secondary transmitted diffraction beams from different positions. The two diffracted beams reach the recording plane at the same time and generate interference fringes on the recording plane. Fig. 4(a) shows the optical path of the experimental setup in this study, which is similar to the classical Young's double-slit experiment, but uses a white laser and a rotating wheel equipped with a band-pass filter. The spatial separation between the two slits is d 0.3 mm. The distance between the double-slit plane and the entrance plane of the CCD is D 200 mm. According to the famous Young's double-slit interference fringe spacing formula$x = D\lambda/d$, the x range of the interference fringe spacing is 0.27 — 0.47 mm when the wavelength is between 405 nm and 700 nm. The Fig. 4(b)—(i) shows the CCD-recorded images of the interference fringes at different wavelengths, and displays the intensity line map and the corresponding interference fringe

contrast υ value, which is defined as (the brightest value of the fringe − the darkest value of the fringe)/(the brightest value of the stripe + the darkest value of a stripe). Except for the wavelengths of 600 nm and 700 nm, the υ of light at other wavelengths is between 0.6 and 0.7. The υ of most wavelengths exceeds 0.7. In addition, the average υ of all wavelengths is 0.77, which meets the requirement of excellent coherence.

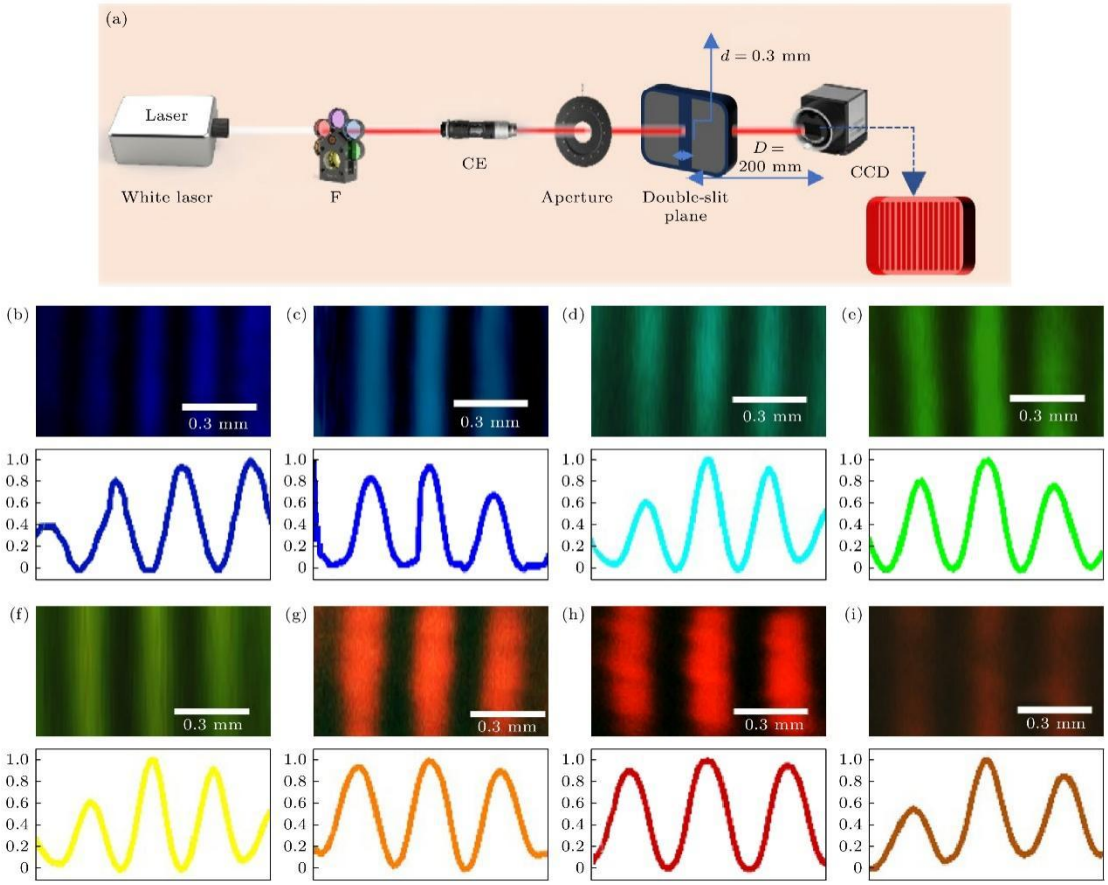

Figure 4. Experimental results in the Young's double-slit experiment: (a) The architecture of Young's double-slit experiment, where F represents rotatable holder embedded with different filters, CE represents collimated beam expanding system; (b)—(i) the interference fringes and intensity line profile of the eight wavelengths, where (b) λ = 405 nm,υ = 0.86; (c) λ = 450 nm, υ = 0.86; (d) λ = 500 nm, υ = 0.75; (e) λ = 532 nm, υ = 0.82; (f) λ = 580 nm, υ = 0.77; (g) λ = 600 nm, υ = 0.62; (h) λ = 635 nm, υ = 0.80; (i) λ = 700 nm, υ = 0.67.

In the eight typical wavelength components selected in the visible band, interference fringes with high contrast are observed in the YDSI system. This shows that white laser has good spatial coherence in the visible range and can be used in areas where coherent white light is required. In addition, combined with the uniform wavefront intensity characteristics of quasi-Gaussian distribution and the consistent linear polarization state of these wavelength components, it can be inferred that although the nonlinear process causes spectral broadening

in the generation process of white laser, it has little effect on the coherence and wavefront quality of the beam. This shows that the white laser retains the excellent beam characteristics of the Ti: sapphire femtosecond laser to a great extent, and shows strong laser spatial coherence. The essence of coherence is the stable amplitude and phase relationship between light waves, so the bandwidth will affect the measurement results. In general, the narrower the bandwidth, the stronger the apparent coherence. Although a filter with a bandwidth of 10 nm is used in this experiment to save cost, which is a relatively wide narrow band, the wavelength components of the white laser still show good spatial coherence under this condition, which has been clearly reflected in the experimental results. The results also indirectly show that if the test is carried out under the condition of narrower bandwidth, it is expected to obtain higher interference fringe contrast, thus showing better spatial coherence.

4. Conclusion

To sum up, in this study, the laser characteristics, especially the spatial coherence, of the high performance white laser developed by our research group were measured in detail. The experimental results show that the developed white laser has excellent performance in many aspects, including ultra-flat spectral distribution (spectral fluctuation is about 1.16 dB in the visible band), high spectral energy (about 14.5 μJ per 10 nm bandwidth), spatial coherence (the average contrast of spatial interference fringes is about 0.77) and polarization characteristics (linear polarization). The measurement of spatial coherence of ultra-broadband and ultra-flat white laser in this study provides important experimental data for the application of white light source, and helps to promote its development. For example, in the field of microscopic imaging, the spectral flatness of the laser, the energy intensity data, and the characteristics of the wavefront intensity of the light wave can provide a reference for the multi-channel confocal microscope, because the device requires a laser source with high intensity, fast wavelength switching, and uniform spot. In the field of tomography, spatial coherence is a key parameter in white-light interferometry. The better the spatial coherence, the higher the measurement accuracy, but the measurement range is reduced accordingly. Different measurement requirements correspond to different coherence requirements, and it is necessary to have a specific grasp of the coherence characteristics of the light source. In the field of holographic imaging, the contrast and polarization of interference fringes are very important. Because the basic principle of holography depends on the recording of interference patterns, the contrast of spatial interference fringes directly affects the quality of reconstructed images, so this parameter has important reference significance for color holography.

Although this kind of white laser with high coherence, ultra-flatness and high intensity has great potential for application and provides a broad space for development in many fields, specific performance data are still needed to make better use of this new laser source. Therefore, the coherence of the self-developed high-intensity, ultra-flat white laser beam is

systematically measured and analyzed in this study, which provides valuable conceptual guidance for the future practical application of white laser in color holography, 3D surface tomography, 3D color display, microscopic imaging and other fields, and will promote the development of related fields.

References

[1] Alfano R R 1990 Appl. Opt. 29 1242

[2] Alfano R R, Shapiro S L 1970 Phys. Rev. Lett. 24 592

[3] Fork R L, Tomlinson W J, Shank C V, Hirlimann C, Yen R, Tomlinson W J 1983 Opt. Lett. 8 1

[4] Froehly L, Meteau J 2012 Opt. Fiber Technol. 18 411

[5] Travers J C, Grigorova T F, Brahms C, Belli F 2019 Nat. Photonics 13 547

[6] Elu U, Maidment L, Vamos L, Tani F, Novoa D, Frozs H, Badikov V, Badikov D, Petrov V, Russell J, Biegert J 2021 Nat. Photonics 15 277

[7] Schliesser A, Picqué N, Hänsch T W 2012 Nat. Photonics 6 440

[8] Udem Th, Holzwarth R, Hänsch T W 2002 Nature 416 233

[9] Petersen C R, Møller U, Kubat I, Zhou B, Dupont S, Ramsay J, Benson T, Sujecki S, Abdel-Moneim N, Tang Z, Furniss D, Seddon A, Bang O 2014 Nat. Photonics 8 830

[10] Jiang X, Joly N Y, Finger M A, Babic F, Wong K L, Travers J C, Russell J 2015 Nat. Photonics 9 133

[11] He P, Liu Y Y, Zhao K, Teng H, He X K, Huang P, Huang H D, Zhong S Y, Jiang Y J, Fang S B, Hou X, Wei Z Y 2017 Opt. Lett. 42 474

[12] Mollenauer L F, Stolen R H, Gordon J P, Tomlinson W J 1983 Opt. Lett. 8 289

[13] Hassan M T, Luu T T, Moulet A, Raskazovskaya O, Zhokhov P, Garg M, Karpowicz N, Zheltikov A M, Pervak V, Krausz F, Goulielmakis E 2016 Nature 530 66

[14] Chen B Q, Ren M L, Liu R J, Zhang C, Sheng Y, Ma B Q, Li Z Y 2014 Light Sci. Appl. 3 e189

[15] Chen B Q, Zhang C, Hu C Y, Liu R J, Li Z Y 2015 Phys. Rev. Lett. 115 083902

[16] Chen B Q, Hong L H, Hu C Y, Li Z Y 2021 Research 2021 1539730

[17] Li M Z, Hong L H, Li Z Y 2022 Research 2022 9871729

[18] Hong L H, Hu C, Liu Y Y, He H J, Liu L Q, Wei Z Y, Li Z Y 2023 PhotoniX 4 11

[19] Hong L H, Liu L Q, Liu Y Y, Qian J Y, Feng R Y, Li W K, Li Y Y, Peng Y J, Leng Y X, Li R X, Li Z Y 2023 Light Sci. Appl. 12 199

[20] Hong L H, Yang H Y, Li Z Y 2023 Research 6 0210

[21] Knapp T, Lima N, Daigle N, Duan S, Merchant J L, Sawyer T W 2024 J. Biomed. Opt. 29 016007

[22] Hassan M A 2025 Appl. Opt. 64 654

[23] Shimobaba T, Ito T 2003 Opt. Rev. 10 339

[24] Kueny E, Meier J, Levecq X, Varkentina N, Kärtner F X, Calendron L 2018 Opt. Express 26 31299

[25] Genty G, Friberg A T, Turunen J 2016 Prog. Opt. 61 71

[26] Melnik M V, Tcypkin A N, Kozlov S A 2018 Rom. J. Phys. 63 203

[27] Zeylikovich I, Alfano R R 2003 Appl. Phys. B 77 265

[28] Su Y B, Fang S B, Gao Y T, Zhao K, Chang G Q, Wei Z Y 2021 Appl. Phys. Lett. 118 261102

[29] Wang P, Huang J, Xie S, Troles J, Russell J 2021 Photon. Res. 9 630

[30] Zhu X, Zhao D, Zhang B, Yang L Y, Yang Y K, Liu S, Hou J 2023 Opt. Express 31 13182

[31] Chang K Y, Chen G Y, Yu H C, Liu J M 2023 Opt. Commun. 533 129281

[32] Feng L B, Lu X, Liu X L, Ge X L, Ma J L, Li Y T, Chen L M, Dong Q L, Wang W M, Teng H, Wang Z H, Sheng Z M, Wei Z Y, He D W, Zhang J 2012 Acta Phys. Sin. 61 174206